Test Rig Development for the Magnetic Bearing's Backup Bearing Contact Forces Measurement during Rotor Drops

Xiao Kang, Alan Palazzolo

Test Rig Development for the Magnetic Bearing's Backup Bearing Contact Forces Measurement during Rotor Drops

Xiao Kang[1], Alan Palazzolo[1*]

ISROMAC 2017

International Symposium on Transport Phenomena and Dynamics of Rotating Machinery

Hawaii, Maui

December 16-21 2017

Abstract

This paper introduces a new catcher bearing (CB) test rig. Compared with the CB test rig described in the previous published literatures, firstly, this test rig eliminates the influence of the motor and coupling on the rotor drop process by implementing a magnetic coupling. The magnetic coupling can make it possible to mechanically pull back the drive motor axially, separating it from the rotating assembly to prevent its influence on the rotor drop. Secondly, the test rig enables the rotor drop contact force measurement in both the horizontal and vertical direction. The implementation of a 3 axis piezoelectric load cell eliminates the measurement error caused by the friction forces on the contact surfaces between the CB housing and the single axis load cells that applied by the former researchers [1,2,9] for the rotor drop force measurement. The 10K Hz sampling frequency of the data acquisition (DAQ) system and the high stiffness of the load cell can also guarantee the accuracy of the force measurement. Thirdly, the tachometers are installed to not only measure the spin speed of the rotor but the spin speed of the catcher bearing inner race. The developed test rig can provide the rotor drop test data to validate the mathematical model of the rotor drop event. Additionally, this test rig is also an essential apparatus for the future experimental research on both the catcher bearing fatigue life estimation, and the catcher bearing damper devices development.

Keywords

Catcher Bearing — Magnetic Bearing — Rotor Drop— Contact Force

[1] *Department of Mechanical Engineering, Texas A&M University, College Station, United States*

***Corresponding author**: a-palazzolo@tamu.edu

INTRODUCTION

The magnetic bearing (MB) has been widely used in the turbomachinery industry. It has the advantages such as a low friction, controllable stiffness and damping [1]. The backup bearing, or catcher bearing (CB), is a crucial part in the magnetic bearing system. It can support the rotor when the magnetic bearing is shut down or malfunctioning due to power loss or other technical failures. When the magnetic bearing suddenly loses power, the rotor with high rotational speed will drop onto the catcher bearing. The large contact force and friction force may impair the catcher bearing or cause large vibrations such as reverse whirls, which may even bring harm to the entire magnetic bearing systems. It is important to both theoretically and experimentally investigate the rotor drop behavior to find better ways to accurately predict the catcher bearing fatigue life and, additionally, prevent large vibrations and contact forces during rotor drops.

The relevant literature [1-5] contains a number of papers that consider the vibration response of a rotating shaft assembly supported by MBs during a MB power outage incident resulting in the sudden drop of the shaft onto the backup (catcher) bearings. Some of these papers compared the predicted and measured vibration displacements of the shaft near the catcher bearings [1-3]. Their comparison of the displacements provides a good means to improve the prediction of displacement motion. Some literatures have investigated the ways to predict the fatigue life of the catcher bearing. Sun et al. [11] used the Lundberg-Palmgren formula to estimate the fatigue life of the CB. Lee et al. [8] expanded the fatigue life calculation of the catcher bearing based on the rain flow counting method together with the Miner's rule and the material's torsional S-N curves. Some researchers also investigated other kinds of catcher bearing. Lahriri et al. [9] numerically and experimentally investigates the pin type catcher bearing. Swanson et al [12] and Kang et al [13] studied the transient response when a rotor drops onto the sleeve type catcher bearing. Kang et al [13] built the 2D dynamic thermal coupled CB model, which enabled the 2D temperature and Von-Mises stress distribution of the CB during rotor drops.

However, catcher bearing life is more directly related to the contact forces exerted on it by the journal during a drop event [1]. Only a very small number of papers have experimentally measured the impact and friction forces during a rotor drop event. Fumagalli et al. [2] obtained the contact force based on the motion of the catcher bearing housing (elastic ring) that is supported by 4 elastic springs. However, their contact forces were obtained indirectly and the calculation accuracy was highly sensitive to the accuracy of the system identification of the housing-spring system. Additionally, the friction force on the contact surfaces between the elastic spring and the CB housing also influenced the accuracy of the contact force measurement, especially for the force in horizontal direction, since the friction force between the rotor and the CB is relatively small compared to the normal contact force. Lahriri et al [9] measured the impact force between the rotor and two types of backup bearings. However, the rotor-bearing contacts in their tests was resulted from the large vibration under resonance conditions or from forced impact excitation,

but not from a free drop onto the catcher bearings. Unlike a true rotor drop the rotor's drop behavior was influenced by the supporting bearings and motor coupling. Saket et al. [10] installed a strain gauge type load measurement system in their catcher bearing system; however, the drop tests were not conducted and only the load cell calibration results were provided.

It can be seen that in the aforementioned papers, the measurement accuracy of the rotor drop contact forces is either influenced by the motor, coupling or the friction force between the catcher bearing housing and the load sensor. To eliminate those influences, the present paper introduces a new catcher bearing test rig, which implements a 3-axis piezo electronic load cell to measure the rotor drop contact force. The 3-axis load cell can capture the contact force in both the horizontal and the vertical directions, so the friction force between the load cell and the CB housing will no longer influence the accuracy of the rotor drop force measurements. Additionally, a magnetic coupling is implemented to connect the drive motor and the rotor. There is an air gap between the two pads of the magnetic coupling as shown in Figure 1. Therefore, before the rotor drops onto the CB, the motor can be pulled back axially and there will be no force and torque transmission between the two pads of the magnetic coupling, so the motor and coupling will no longer influence the rotor drop events. Moreover, the vibration of the shaft, the spin speed of the rotor and the catcher bearing inner race can also be monitored. Furthermore, the paper experimentally investigated the influence of rotor dropping with different spin speed, especially of the rotor drops with the spin speed higher than its critical speed. The test rig enables the investigations of the catcher bearing fatigue life and the catcher bearing damper devices in the future.

1. TEST RIG DESCRIPTION

Figure 1 shows a diagram of the catcher bearing (CB) test rig when the rotor drops onto the CB. The photo of the real catcher bearing test rig is shown in Figure 3. In this rig, the rotor is initially supported by a tapered roller bearing and a self-aligning bearing. The drop test is initiated when the drive motor is mechanically pulled axially backwards， separating it from the rotating assembly and in this process the gap in the magnetic coupling that connects the motor and rig rotor is suddenly thrust open. Next, the outer race of the tapered roller bearing is pushed forward by a solenoid-spring system， opening a clearance in the bearing to let the rotor drop freely onto the catcher bearing, where the tapered roller bearing and the self aligning bearing are shown in Figure 2.

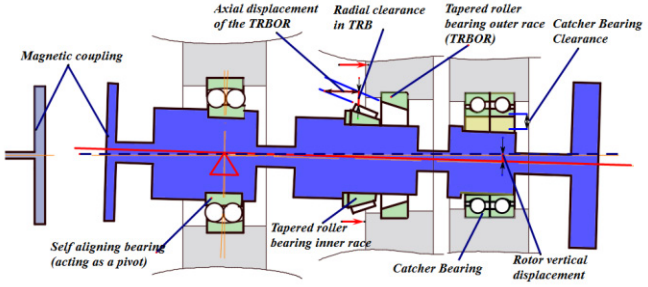

Figure 1. Scheme plot of the way to let rotor drop onto the CB

(a) (b)

Figure 2. (a) Self aligning bearing (b) Tapered roller bearing

From Figure 2. it can be seen that the outer race of the tapered roller bearing can be separated from its inner race and rollers. The inner race of the self aligning bearing can rotate freely so it can act as a pivot during the rotor drop and has limited influence on the rotor drop process.

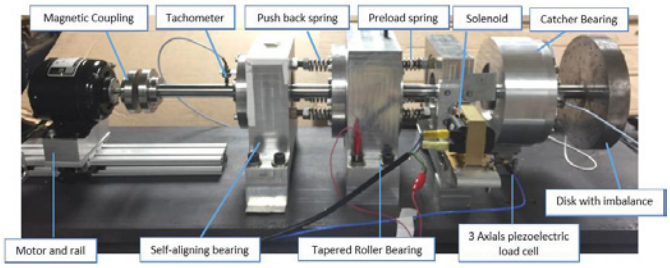

Figure 3. Catcher bearing test rig

A disk with balancing holes is installed on the non drive end of the rotor as shown in Figure 3. A 3-axis piezoelectric load cell is installed under the catcher bearing housing to measure the impact forces on the catcher bearing during rotor drops. The high stiffness of the load cell and its support and the 10 kHz DAQ sampling rate yield highly accurate measurements in both the horizontal and vertical directions. Here the duplex pair of the angular contact ball bearings is working as the catcher bearing. The data acquisition system is shown in Figure 4.

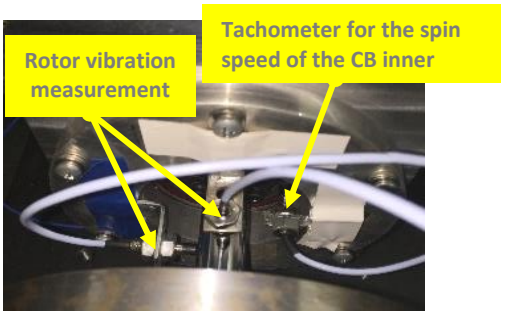

(a)

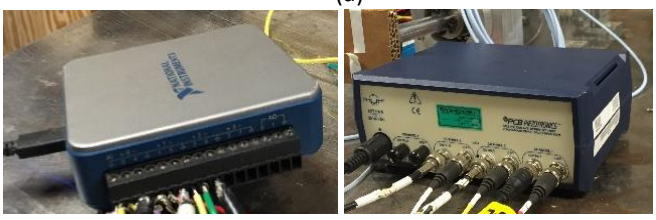

(b) (c)

Figure 4 . Data acquisition system of the Catcher Bearing test rig. (a) Bently eddy current sensors (b) NI USB DAQ board (c) Load cell signal conditioner

Two eddy current sensors (Bently Nevada 3300XL probe) are placed near the catcher bearing location, measuring the displacement of the rotor during rotor drop. Because the sensors are fixed onto the housing, the measured rotor displacements are relative to the housing. Two eddy current sensors (Bently Nevada 3300XL probe) are working as tachometers to measure the spin speeds of the rotor and the

catcher bearing inner race. The Labview based data acquisition software is used to monitor and save the measured vibration and force information.

1.1 Rotor free drop test

Because the drop test is initiated by separating the inner and outer race of the tapered roller bearing to create the clearance, it is essential to make sure that during rotor drops, the radial clearance in the tapered roller bearing is always larger than the displacement of the rotor. Then the rotor can drop freely without the influence of the tapered roller bearing. Thus, the rotor free drop test is conducted as shown in Figure 5.

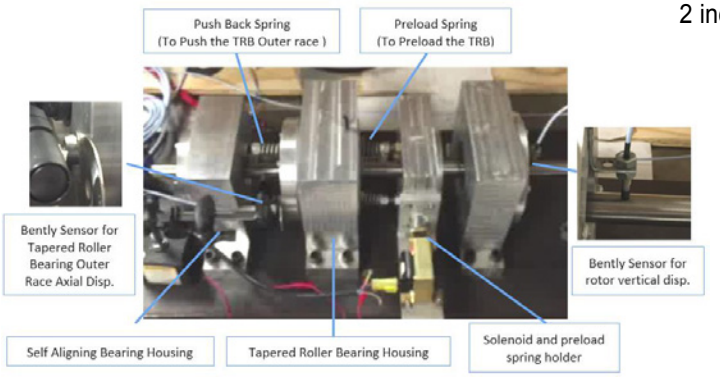

Figure 5. Rotor free drop test

One Bently sensor (Bently Nevada 3300XL probe) measures the axial displacement of the tapered roller bearing outer race (TRBOR). Another Bently sensor (Bently Nevada 3300XL probe) measures the vertical displacement of the rotor near the catcher bearing location. The radial clearance in the tapered roller bearing can be obtained by the equation (1). The TRBOR's axial displacement, radial clearance and rotor's vertical displacement are also shown in the Figure 1.

$$C_{TB} = A_{TPOR} \tan(\alpha_{TP}) \quad (1)$$

where the C_{TP} is the radial clearance in the tapered roller bearing; the A_{TPOR} is the axial displacement of the tapered roller bearing outer race; and α_{TP} is the contact angle of the tapered roller bearing. The comparison between the radial clearance of the tapered roller bearing and the rotor drop displacement is shown as Figure 6.

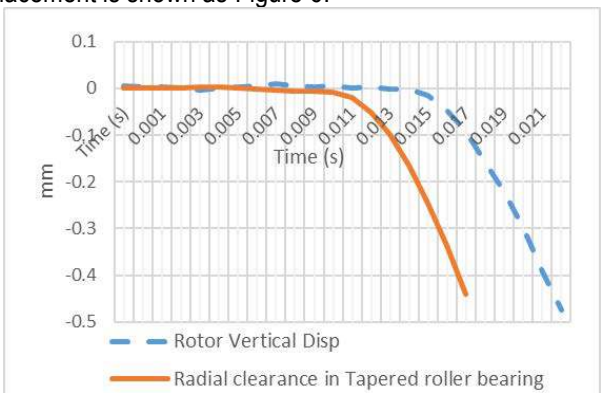

Figure 6. Rotor vertical displacement and the radial clearance between the tapered roller bearing inner and outer race

From Figure 6 it can be seen that when the tapered roller bearing outer race is pushed away, the radial clearance in the tapered roller bearing is alwasys larger than the vertical displacement of the rotor. Therefore, the rotor drop process will not be influenced by the tapered roller bearing. The rotor can drop freely.

1.2 Load cell calibration for the impact force measurment

The 3-axis piezoelectric load cell has been precisely calibrated by the manufacturer for the attached static and harmonic dynamic load. To make sure the 3-axis piezoelectric load cell can also effectively capture the impact force, vertical impact tests are applied. As shown in Figure 7, a spring with the stiffness of 1.926e5N/m (obtained from the manufacturer) is fixed on the load cell by a pin. A steel cube with the mass of 544g is dropped on to the spring with different heights (1 inch, 2 inches and 3 inches).

Figure 7 Impact force calibration test

There are more than 15 tests are made for each height to verify the tests' repeatability. The measured forces and the predicted forces are compared as following. When the drop height is 1inch, the prediction and measurement are in Figure 8, where Figure 8 a is the comparison of the force amplitude among all the tests and the prediction. Figure 8 b and c are the transient force response of the prediction and the highlighted test.

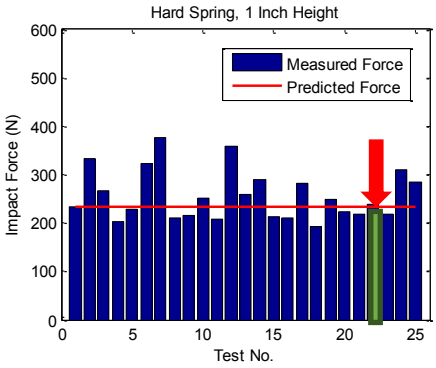

(a) Force amplitudes of different tests

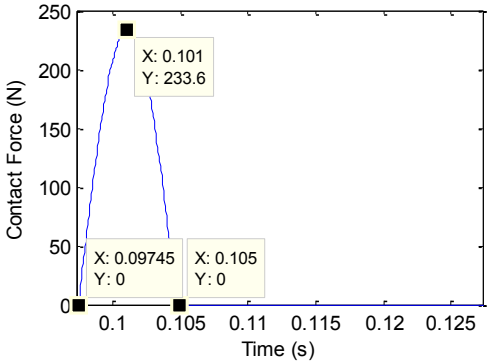

(b) Predicted transient force response

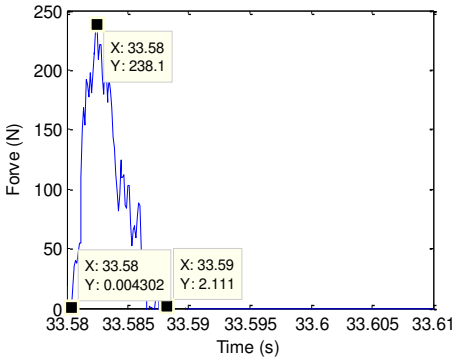

(c) Measured transient force of the highlighted drop test

Figure 8 . Drop from 1 inch (25,4mm) height

From Figure 8 (a), the predicted force is similar to 80% of the drop cases (within 10% differences). A few cases (20%) have the contact forces 100N (40%) larger than the predicted value. The transient force response of the highlighted case is compared with the predicted transient response. The results show the duration of the forces are both around 0.007s. Note the force duration of both Figure 8 (b) and Figure 8 (c) are 0.03s. When the drop height is 2 inches, the measured forces and predicted forces are shown in Figure 9.

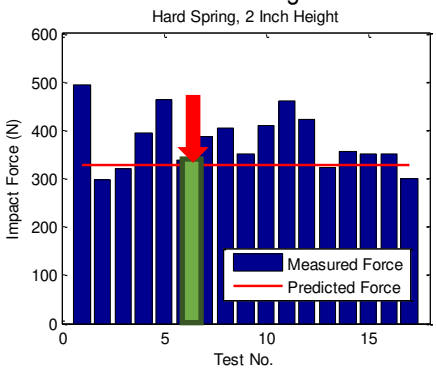

(a) Force amplitudes of different tests

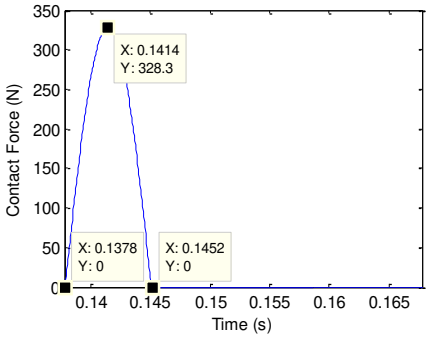

(b). Predicted transient force response

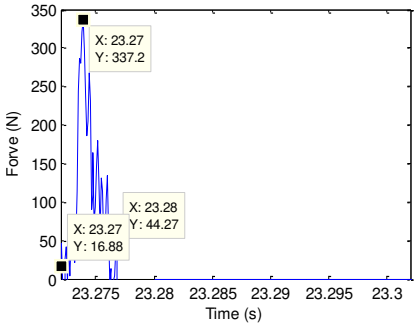

(c). Measured transient force of the highlighted drop test

Figure 9. Drop from 2 inch height

In Figure 9, the predicted force is similar to 70% of the drop cases (with 10% differences). A few cases (20%) have the contact forces 100N (30%) larger than the predicted value. The transient force response of the highlighted case is compared with the predicted transient response. The results show the duration of the forces are both around 0.007s, while the duration of the measured force is a little bit smaller. When the drop height increases to 3 inches, the results are shown in Figure 10.

From Figure 10 (a), the predicted force is similar to 75% of the drop cases (with 10% differences). A few cases (18%) have the contact forces 100N (40%) larger than the predicted value. The transient force response of the highlighted case is compared with the predicted transient response. The results show the time duration of the forces is around 0.007s. While there are several impacts for the measured force.

(a) Force amplitudes of different tests

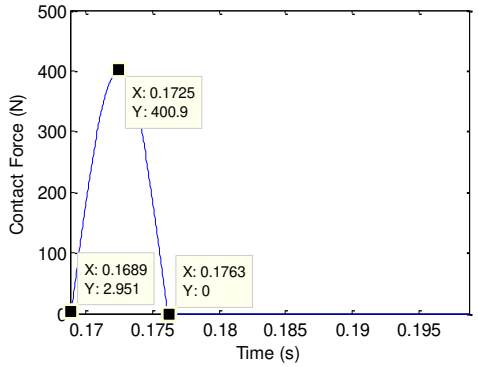

(b). Predicted transient force response

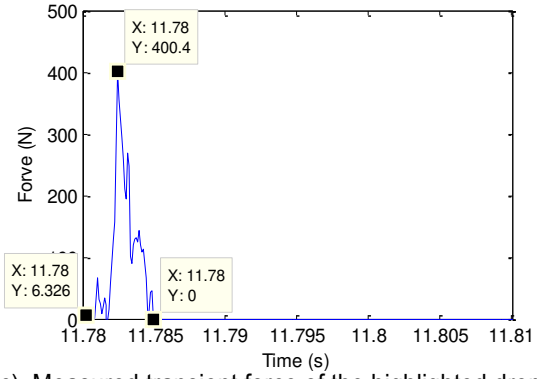

(c). Measured transient force of the highlighted drop test

Figure 10. Drop from 3 inch height

Thus, with different drop heights, 70% of the measured force amplitudes are within 10% of the predicted force. Therefore, the load cell is reliable for the impact force measurement.

2. TEST RESULTS

In this rotor drop test, the initial rotor drop spin speed is 2444 RPM which is larger than the rotor's first critical speed (1500 RPM). Due to the limitation of the transmission rate of the current NI DAQ board, the sampling frequency for both the vibration and force information is 3300Hz. The rotor geometry information is shown as Figure 11.

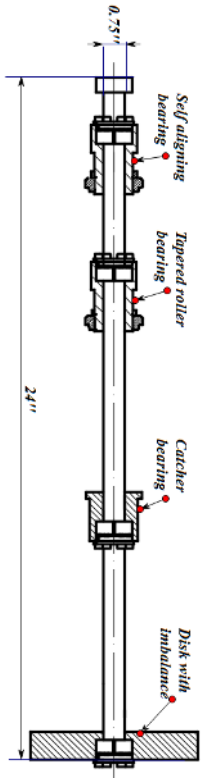

Figure 11. Geometry of the test rotor

The measured rotor orbit at the sensor's location is shown in Figure 12.

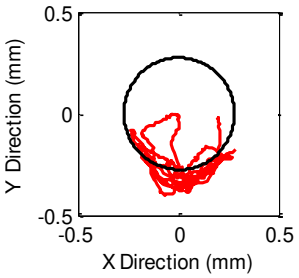

Figure 12. Measured rotor drop orbit

Figure 12 shows that the rotor vibrates on the bottom of the CB after a few initial bounces. The time history of the translation motions of the rotor center at the sensor's location are shown in Figure 13.

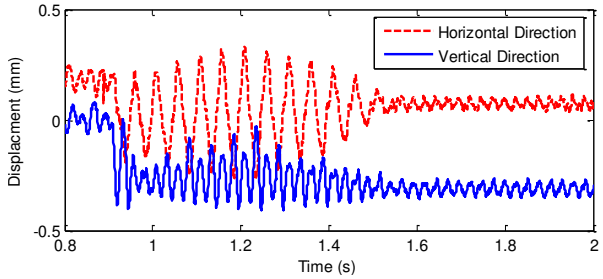

Figure 13. Translational motions of the rotor center at the sensor's location

The measured contact forces during rotor drops are shown in Figure 14.

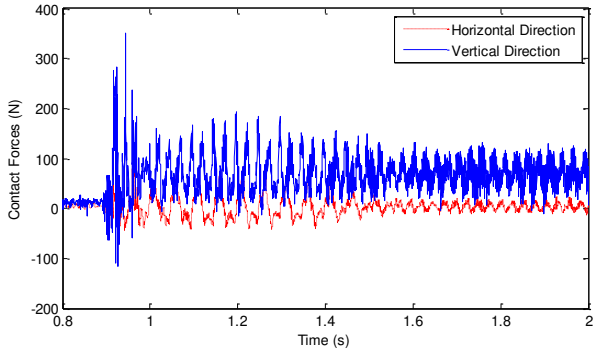

Figure 14. Measured contact forces during rotor drops

Figure 14 shows that the 3 axes piezoelectric load cells can effectively capture the contact forces in both the horizontal and vertical directions simultaneously. The first few hits have higher contact forces and those contact forces are about 5 to 6 times larger than the static load acting on the CB, which is about 60N based on the initial test. Then the vertical contact forces vibrate around 60N which is caused by the rotor's vibrations. The spin speed of both the rotor and the catcher bearing inner race (CBIR) are measured as Figure 15.

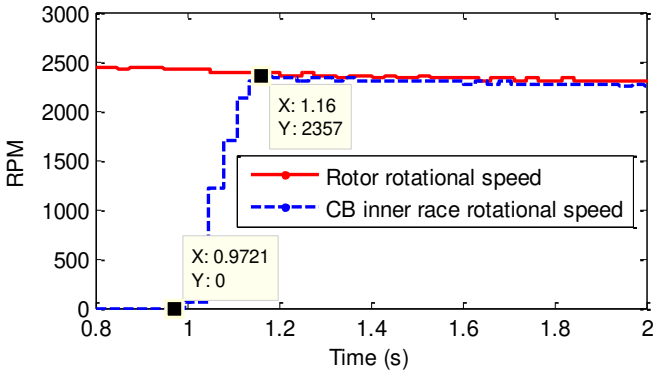

Figure 15. Measured rotational speed of the rotor and CBIR

Figure 15 shows that the rotational speed of the rotor starts to decay when the rotor contacts the CB. It takes about 0.2s for the CBIR to reach a similar rotational speed as the rotor, while the rotational speed of the CB is slightly lower than the rotor. This is because the CBIR has a larger radius than the rotor.

3. INFLUENCE OF THE ROTATIONAL SPEED

Rotor drop tests with different spin speeds are also conducted. The rotor orbits that with different spin speeds can be found in Figure 16. The tested three spin speeds are 593.6RPM, 1139 RPM and 2444 RPM, while the first critical speed of the rotor is about 1500 RPM according to the initial test. The goal it to observe the influence of rotor dropping with the spin speed higher than the rotor's critical speed and how the rotor drop spin speed influence the rotor drop behavior.

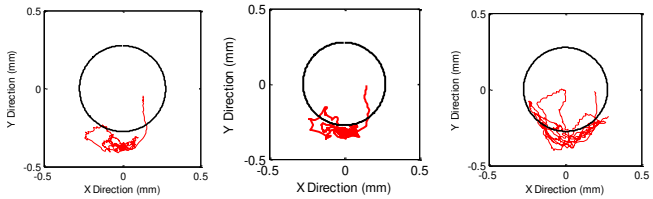

(a)594.6 RPM test (b) 1139 RPM test (c) 2444 RPM test

Figure 16. Rotor orbit with different spin speeds

To better observe how the rotor's drop spin speed influences

the rotor drop behavior, here the time span is chosen as 0-25s. The rotor spin speeds and contact forces during 0-25s is shown as Figure 17. Note the first critical speed of the rotor is about 1500RPM, so from Figure 17 we can also observe the rotor transient response when it passes through its critical speed.

From Figure 17 (a), it can be seen that when rotor drop spin speeds get higher, it will take longer time to let the rotor stop spinning. From Figure 17 (b), it can be seen that for the first few hits, higher drop spin speeds do not results in higher contact force. This is because the contact forces for the first few hits are highly related to the initial drop conditions, while from the Figure 17 (d) and (f), they show for the rest hits, higher rotational speeds will result in higher contact forces. This may be caused by the residual imbalance of the rotor. Although the rotor is balanced for these cases, there is still some minor residual imbalance (within 5e-5 kg.m). The spin speed contributes much to the imbalance force of the rotor and causes higher contact forces.

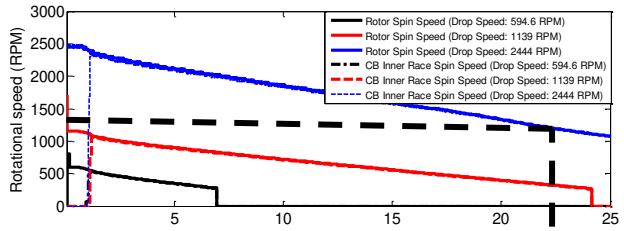

(a) Spin speeds of rotors and catcher bearing inner races

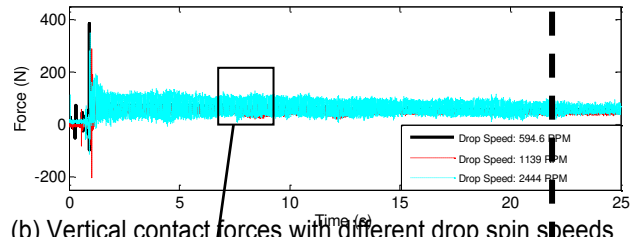

(b) Vertical contact forces with different drop spin speeds

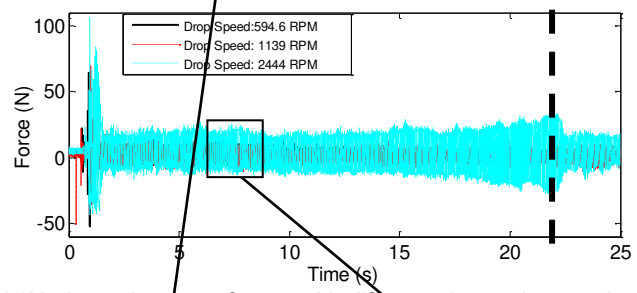

(c)Horizontal contact forces with different drop spin speeds

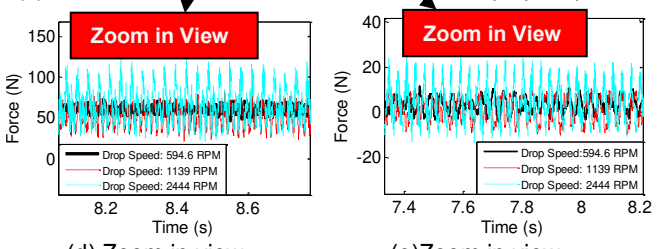

(d) Zoom in view (e)Zoom in view

Figure 17. Test results of rotor drop with different spin speeds

Additionally, it can be seen from Figure 17 (c) that when rotor passes its critical speed, the contact forces is greatly increased which is due to the large vibration caused by the resonance. So the rotor critical speed is also needed to be considered for the catcher bearing design.

CONCLUSION

A catcher bearing test rig is developed which can measure the rotor's vibration, catcher bearing contact force and the spin speeds of the catcher bearing inner race.

For the influence of rotor drops with different spin speeds, the results show that for the first hit, high spin speed doesn't necessarily cause higher contact force, because the contact force for the first few hits are highly related to the initial drop conditions. While for the rest hits, higher rotational speeds will result in higher contact forces. It may be caused by the residue imbalance of the rotor. Though the rotor is balanced for these cases, there may still be some residual imbalance. The spin speed will contribute much to the imbalance force of the rotor and finally results higher contact forces.

Additionally, when rotor passes its critical speed, the contact forces are greatly increases which is due to the large vibration caused by the resonance. Therefore, the rotor critical speed is also need to be considered for the catcher bearing design.

Future tests with varying surface roughness and other parameters such as rotor imbalance and catcher bearing clearance will be performed to investigate the approaches to mitigate the reverse whirl.

Future tests will also include different types of dampers to investigate their effect in preventing the reverse whirl and reducing the contact forces.

ACKNOWLEDGMENTS

This research was supported by the Turbomachinery Research Consortium (TRC) at Texas A&M University. Special thanks to Mr. Erwin Thomas, Mr. Xiaojun li, Mr. Xiaomeng Tong and Mr. Stephen Farris for their assistance in the construction of the rig and the DAQ system..

REFERENCES

[1] Gerhard Schweitzer. Eric H. Maslen. Magnetic Bearings Therory, Design, and Application to Roating machinery. Springer, London, 2009

[2] M. Fumagalli. Modelling and measurement analysis of the contact interaction between a high speed rotor and its stator. PhD thesis, ETH Zurich No 12509, 1997.

[3] M. Helfert. Rotorabsturze in Walzlager - Experimentelle Untersuchungen des Rotor-Fanglager-Kontakts, PhD thesis, TU Darmstadt, Fachgebiet Mechatronik im Maschinenbau, 2008.

[4] Gelin A , Pugnet JM , Hagopian J D. Dynamic behavior of flexible rotors with active magnetic bearings on safety auxiliary bearings. Lyon, France: Proceedings of 3rd International Conference on Rotor dynamics, 1990. 503-508.

[5] Ishii, T., and Kirk, R. G., 1996, "Transient Response Technique Applied to Active Magnetic Bearing Machinery During Rotor Drop," ASME J. Vibr. Acoust., 118, pp. 154–163.

[6] Sun, G., Palazzolo, A., Provenza, A., and Montague, G., 2004, "Detailed ball bearing model for magnetic suspension auxiliary service," Journal of sound and vibration, 269(3), pp. 933-963.

[7] Sun, G., 2006, "Rotor drop and following thermal growth simulations using detailed auxiliary bearing and damper models," Journal of sound and vibration, 289(1), pp. 334-359.

[8] Lee, J. G., and Palazzolo, A., 2012, "Catcher bearing life

prediction using a rainflow counting approach," Journal of tribology, 134(3), p. 031101.

[9] Said Lahriri, Ilmar F. Santos. Experimental quantification of dynamic forces and shaft motion in two different types of backup bearings under several contact conditions. Mechanical System and Signal Processing. 2013.

[10] Fawas Y Saket, M. Necip Sahinkaya, Patrick S. Keogh. Touchdown Bearing Contact Forces in Magnetic Bearing Systems. Proceedings of ASME Turbo Expo 2013: Turbine Technical Conference and Exposition GT2013. June 3-7, 2013, San Antonio, Texas, USA

[11] Sun, G., Auxiliary Bearing Life Prediction Using Hertzian Contact Bearing Model, Journal of Sound and Vibration., 128,pp. 203-209

[12] Swanson, E.E., Raju, K.V.S., Kirk, R.G. Test Results And Numerical Simulation Of AMB Rotor Drop. Proc. 6th Int'l Conf. on Vibrations in Rotating Mach., IMechE, pp. 119-131.

[13] Xiao Kang, Alan Palazzolo. Dynamic and Thermal Analysis when Rotor Drop on to the Sleeve Type Catcher Bearings. Proceedings of ASME Turbo Expo 2017: Turbine Technical Conference and Exposition GT2017. June 26-30, 2017, Charlotte,NC, USA